LA-UR-86-1548

RECEIVED BY OSTI JUN 06 1986

CONF-860810--6

Los Alamos National Laboratory is operated by the University of California for the United States Department of Energy under contract W 7405-ENG-36

LA-UR--86-1548

DE86 011264

TITLE: LIQUID METAL THERMOACOUSTIC ENGINE

AUTHOR(S): G. W. Swift, A. Migliori and J. C. Wheatley

SUBMITTED TO Intersociety Energy Conversion Engineering Conference, San Diego, CA, August 25-29, 1986

## DISCLAIMER



Los Alamos Los Alamos National Laboratory
Los Alamos, New Mexico 87545

MASTER

# LIQUID METAL THERMOACOUSTIC ENGINE

G. W. Swift, A. Migliori, J. C. Wheatley
Condensed Matter and Thermal Physics Group
Los Alamos National Laboratory,
Los Alamos, NM 87545

## ABSTRACT

We are studying a liquid metal thermoacoustic engine both theoretically and experimentally. This type of engine promises to produce large quantities of electrical energy from heat at modest efficiency with no moving parts. The only motion is associated with acoustic oscillations in the liquid metal. It is a new concept in energy conversion.

A sound wave is usually thought of as consisting of pressure oscillations, but always attendant to the pressure oscillations are temperature oscillations. The combination produces a rich variety of "thermoacoustic" effects. These effects are usually so small that they are never noticed in everyday life; nevertheless under the right circumstances they can be harnessed to produce powerful heat engines, heat pumps, and refrigerators. In our liquid metal thermoacoustic engine, heat flow from a high temperature source to a low temperature sink generates a high-amplitude standing acoustic wave in liquid sodium. This acoustic power is converted to electric power by a simple magnetohydrodynamic effect at the acoustic oscillation frequency.

We have developed a detailed thermoacoustic theory applicable to this engine, and find that a reasonably designed liquid sodium engine operating between 700°C and 100°C should generate about 60 W/cm$^2$ of acoustic power at about 1/3 of Carnot's efficiency. Imperfect efficiency results equally from three sources: the viscosity of the sodium, the nonzero thermal conductivity of the sodium and the metal parts of the engine, and the intrinsic irreversibility characteristic of this kind of engine and caused by an oscillatory diffusion of heat across a temperature difference at the acoustic frequency. Construction of a 3000 W-thermal laboratory model engine has just been completed, and we have exciting preliminary experimental results as of the time of preparation of this manuscript showing, basically, that the engine works! We have also designed and built a 1 kHz liquid sodium magnetohydrodynamic generator and have finished extensive measurements on it. It is now very well characterized both experimentally and theoretically. The first generator of its kind, it already converts acoustic power to electric power with 40% efficiency with understandable electrode resistance and end effects responsible for nearly all the losses.

THE EARLIEST THERMOACOUSTIC ENGINE that is a direct antecedent of the engine described here is the Sondhauss tube (1*), which was studied quantitatively at least as early as 1850 and explained qualitatively by Lord Rayleigh (2) some years later. In the early Sondhauss tube, a hot glass bulb attached to a cool glass tubular stem was observed to emit sound. Lord Rayleigh emphasized in his qualitative explanation the importance of the relative phasing between thermodynamic effect (temperature change) and motion, this phasing being produced by the thermal time lag between the gas and the surrounding walls. More recently, Feldman (3) has reviewed some of the qualities of Sondhauss tubes and emphasized the importance to the performance of inserting certain structures into the tube. Then, beginning in 1969, Rott and coworkers (4-11) wrote a series of papers on thermoacoustics that put thermoacoustics in gases on a sound theoretical footing. More recently, we (12-14) have made a number of quantitative experimental and theoretical studies of thermoacoustic phenomena in gases in resonant tubes containing certain internal structures. Our gas work provides both a conceptual and an experimental basis for the present study.

Over 50 years ago, Malone (15) demonstrated for the first time that reciprocating heat engines using liquid water as the primary working fluid can be effective and efficient prime movers. Malone realized the liquid sodium, among other liquids, would be a suitable substance thermodynamically, but that "sodium and potassium and alloys of them are too dangerous." For his purpose, Malone was undoubtedly right in selecting liquid water, but in the light of modern technology, probably wrong in the assessment of the practical use of liquid sodium, potassium, and their eutectic alloy NaK. Thermodynamically Malone's judgment about the liquid alkali metals was quite right. In heat engines using fluids, especially acoustic engines, there are two dimensionless thermodynamic quantities of primary importance. One is the quantity $T\beta$, where $T$ is absolute temperature and $\beta$ is the isobaric expansion coefficient, because the isothermal heat flows in response to pressure changes are proportional to this factor. The second is the quantity $\gamma-1$ where $\gamma$ is the ratio of the isobaric to the isochoric specific heat. The effective motion in acoustic engines in response to a pressure change is proportional to the difference between the isothermal and adiabatic compressibilities, which is itself proportional to $\gamma-1$; hence, the work flow from the engine is proportional to $\gamma-1$. For gases $T\beta = 1$ while the quantity $\gamma-1$ is 2/3 for monatomic gases and of order 0.4 for gases like air at moderate temperatures. For sodium at a temperature of 700°C, which might be in the middle of the temperature range of a high-power liquid-sodium acoustic engine as described below, $T\beta = 0.28$ and $\gamma-1 = 0.43$. There is a general tendency for these parameters to increase with increasing temperature, but overall changes are not large. Hence liquid sodium is a good fluid thermodynamically, especially at high temperatures. Another important quality of a liquid as opposed to a gas in an acoustic engine is that for a given Mach number the power density is proportional to $\rho a^3$, where $\rho$ is the density and $a$ is the sound velocity. Comparing liquid sodium

*Numbers in parentheses designate References at end of paper.

t 700°C with gaseous $^4$He at 23 bar and 700°C, the ower density is 1000 times higher in the case of iquid sodium; thus for a high power density, Mach umbers for sodium can be small enough that a linear heory is appropriate, even though pressure ampli- udes can be extremely high, limited only by the trength of the resonator case. What is particularly mportant for liquid sodium working in an acoustic ngine, given that its thermodynamic properties re adequate, is that its Prandtl number $\sigma = \nu/\kappa$, here $\nu$ is kinematic viscosity and $\kappa$ is thermal iffusivity, is so very low: 0.004 at 700°C as against /3 for $^4$He gas. This means that a liquid-sodium coustic engine is acoustically nearly ideal (13,14), that the thermodynamic processes on which the ngine is based are largely controlled by thermal onduction while viscous losses can be made propor- ionally much smaller relative to work flows than hose in a gas engine. The Prandtl number is low wing to a large electronic thermal conductivity hile the viscosity, due to motion of sodium atoms, more "normal." Another practical feature of odium is that its substantial electrical conducti- ity, of order 0.1 that of copper, makes it possible o use Faraday emf's and currents, generated magneto- ydrodynamically at the audio frequency of the ngine, to generate ac electrical power without the eed for moving parts or seals.

A possible general schematic form of a liquid odium acoustic engine, omitting all difficult echnical features, is shown in Fig. 1. The funda- ental acoustic resonance of the liquid sodium in his pressure vessel or resonator has a pressure ntinode at each end, a velocity antinode at the entral region, and corresponds effectively to a alf wavelength in the tube. At a suitable location n the tube, we place a stack of plates S made from material having, relative to liquid sodium, both a igh product of heat capacity and thermal conducti- ity and a high acoustic impedance. By means of uitable heat-exchange conduits, indicated by little ircles at appropriate ends of each plate, the ends f S are maintained at hot and cold temperatures $T_H$ nd $T_C$ as shown, with $T_H$ adjacent to the nearest obe end. The liquid sodium in the tube will scillate spontaneously and cause a time-averaged ork $\dot{W}$ to flow out of the device when the imposed atio of $T_H$ to $T_C$ is high enough, while time- veraged heat $\dot{Q}_H$ flows in at $T_H$ and $\dot{Q}_C$ flows ut at $T_C$. Such spontaneous oscillations are a onsequence, in part, of having the correct phasing etween the sinusoidally oscillating temperatures and

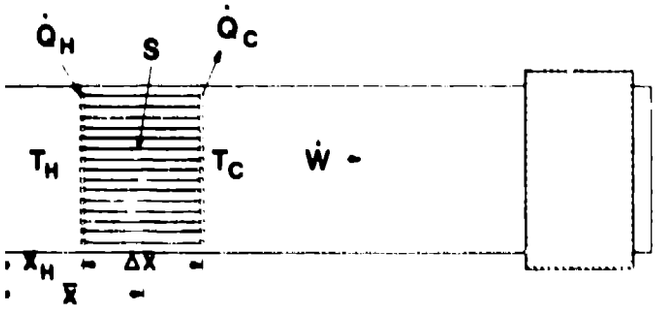


ig. 1 - Shown is a schematic representation of a liquid-sodium acoustic engine, with the essential parts required for a complete working system. These are the heat exchangers at the ends of the stack, the stack S, a resonant tube, and some means for extracting work, here represented by the shaded box on the right.

motion of the fluid. Suitable phasing is achieved both by the magnitude of the longitudinal tempera- ture gradient imposed on S and by the natural process of lateral thermal conduction between fluid and plates. The acoustic work flow $\dot{W}$ is then converted to useful power, such as electric power, by some means such as a magnetohydrodynamic (mhd) transducer.

## THEORY OF THE THERMOACOUSTIC ENGINE

The theory behind the thermoacoustic engine is very simple conceptually, although it is very tedious to work out all the details (16). Consider a paral- lel plate geometry as shown in Fig. 1, with the x-axis along the direction of sound propagation and the y-axis perpendicular to the planes of the parallel plates. We write down an equation of motion for the fluid

$$\rho \frac{\partial \vec{v}}{\partial t} = -\vec{\nabla}P + \rho\nu\nabla^2\vec{v} \quad , \tag{1}$$

with the boundary condition $\vec{v} = 0$ at the fluid-plate interface, and a continuity equation for the fluid,

$$\frac{\partial \rho}{\partial t} + \vec{\nabla}\cdot(\rho\vec{v}) = 0 \quad , \tag{2}$$

where $\vec{v}$ is velocity and P is pressure. We require the fluid's isobaric specific heat $c_p$, its thermal expansion coefficient $\beta$, its ratio of isobaric to isochoric specific heats $\gamma$, and its sound speed a, so that we can use the relations

$$ds = \frac{c_p}{T} dT - \frac{\beta}{\rho} dP \quad , \tag{3}$$

$$d\rho = -\rho\beta dT + \frac{\gamma}{a^2} dP \quad , \tag{4}$$

where T is temperature and s is entropy. Finally, we write down equations for heat flow in the fluid and solid

$$\rho T\left(\frac{\partial s}{\partial t} + \vec{v}\cdot\vec{\nabla}s\right) = \vec{\nabla}\cdot(k\vec{\nabla}T) \quad , \tag{5}$$

$$\rho_{sol} c_{sol} \frac{\partial T_{sol}}{\partial t} = k_{sol}\nabla^2 T_{sol} \quad , \tag{6}$$

where k is thermal conductivity, and use the boundary conditions $T = T_{sol}$ and $k\partial T/dy = k_{sol}\partial T_{sol}/dy$ at the fluid-solid interface. We then linearize these equa- tions by assuming that all variables oscillate at angular frequency $\omega$:

$$P = P_m + P_1(x)e^{i\omega t} \quad , \tag{7}$$

$$\rho = \rho_m(x) + \rho_1(x,y)e^{i\omega t} \quad , \tag{8}$$

$$\vec{v} = \hat{x}\, u_1(x,y)e^{i\omega t} + \hat{y}\, v_1(x,y)e^{i\omega t} \quad , \tag{9}$$

$$T = T_m(x) + T_1(x,y)e^{i\omega t} \quad , \tag{10}$$

$$T_{sol} = T_m(x) + T_{1,sol}(x,y)e^{i\omega t} \quad , \tag{11}$$

$$s = s_m(x) + s_1(x,y)e^{i\omega t} \quad . \tag{12}$$

We then manipulate (16) the resulting equations into the form of a wave equation for $P_1(x)$ in terms of $\partial T_m/\partial x$ and material properties and geometry, and equations for enthalpy and acoustic power fluxes along x in terms of $P_1(x)$, $T_m(x)$, material properties, and geometry. The equations described above can be solved numerically self-consistently to find all the thermal and acoustic quantities of interest. In general, we find that for sufficiently large $\partial T_m/\partial x$ and in the presence of an acoustic standing wave,

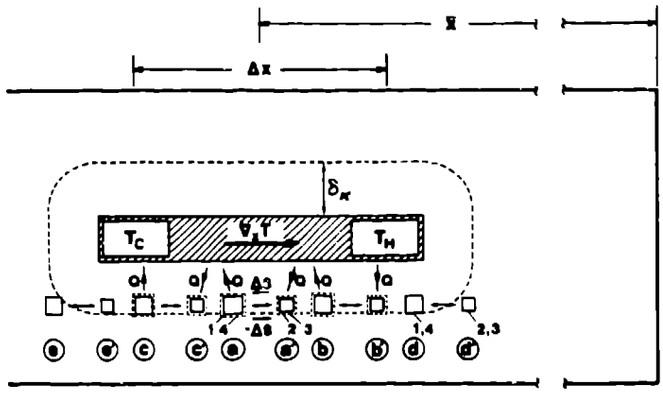


Fig. 2 - Shown is one plate of an acoustic engine in which the important lengths for heat transfer and fluid displacement are exaggerated. The transport of entropy, as explained in the text, occurs in the region of gas approximately one thermal penetration depth $\delta_\kappa$ from the plates. Parcels of gas, represented by the boxes, are compressed, expanded, and displaced by the acoustic pressure variations, and exchange heat with the plates.

there is an acoustically stimulated heat flow down the temperature gradient and real acoustic power is thereby produced at the frequency of the standing wave.

The basic principles of these two phenomena can be understood by considering Fig. 2, where we show in cross section a single plate in a resonator. For heuristic purposes we will assume that the fluid is inviscid and that thermal conduction along x is negligible. Figure 2 is a longitudinal section through the plates and the confining tube or pressure vessel for the fluid. Only one plate from the stack of plates S is shown, because in a boundary-layer approximation the processes in all plates will be similar. This plate, shown cross-hatched, has geometrically ideal heat exchangers at each end consisting of two cavities labeled $T_H$ and $T_C$ in the plate. Heat-exchange fluids at these temperatures flow through these cavities. As a consequence of this heat exchange, a temperature gradient $\nabla_x T$ is set up in the plate in the direction shown. Here we will assume that the length of the plate is short enough that average values suffice to describe not only $\nabla_x T$ but also the several parameters depending on $T_m$ that describe the system, such as $T_m\beta$, $\gamma-1$, a, $\rho_m$, $\kappa$, etc. The dotted line around the plate is drawn to be one thermal penetration depth $\delta_\kappa = (2\kappa/\omega)^{1/2}$ from the surface of the plate. The various squares drawn near the plate and labeled (a), (b), etc., are all parcels of fluid that communicate thermally with the plate during at least a part of a cycle. We show five parcels and their extremes of position. Thus (a) and (a′) represent, respectively, the maximum expanded and maximum compressed positions of parcel (a) and similarly for (b) and (b′), and (c) and (c′), (d) and (d′), and (e) and (e′). It will further facilitate understanding if we replace the true sinusoidal cyclic motion of a parcel by an articulated cycle, indicated typically for parcels (a) and (d), and simply say that for parcels within $\delta_\kappa$ of the plate thermal contact is achieved while for parcels outside that distance there is no heat exchange with the plate. Then the articulated cycle for parcel (a) consists of a rapid motion (1→2) from (a) to (a′) with no heat flowing, a wait (2→3) at (a′) for thermal equilibrium with the plate, a rapid motion (3→4) from (a′) to (a) in which no heat flows, followed by a wait (4→1) again for thermal equilibrium, etc. The cycle is 1,2,3,4,1,.... The thermal time lags required for heat conduction in the articulated cycle correspond to the phase difference between temperature and motion in the sinusoidal cycle.

We first consider the concept of hydrodynamic entropy flow in the fluid. As the parcel moves rapidly from (a) to (a′) on the 1→2 part of the cycle, let us say that it is translated a distance $2x_1$ toward the closed end while its pressure is increased by $2P_1$ and its temperature by $2T_{1,ad}$, where $T_{1,ad} = T_m\beta P_1/\rho_m c_p$. Now if $\partial T_m/\partial x$ is sufficiently large, the parcel at (a′) will find itself laterally adjacent to a point on the plate that is hotter than it is and heat Q will flow from the plate to the parcel, as shown in Fig. 2, adding ΔS to its entropy and increasing its volume from 2 to 3. In part 3→4 of the cycle, the parcel moves $2x_1$ from the closed end, its pressure dropping by $2P_1$ and its temperature dropping by $2T_{1,ad}$. The parcel at (a) will find itself laterally adjacent to a point on the plate which is colder than it is, and heat Q flows from parcel to plate, decreasing the parcel's entropy by ΔS and decreasing its volume from 4→1. It is clear from this discussion, as suggested in detail in Fig. 2, that as the parcel moves rapidly (isentropically) from (a) to (a′) in 1→2 an entropy decrement is transported by the parcel; while as it moves rapidly from (a′) back to (a) in 3→4 an entropy increment is transported. The net effect is a hydrodynamically or convectively transported entropy 2ΔS each cycle from right to left. After multiplication by T we have an acoustically stimulated hydrodynamic heat flow. The same remarks could be made of parcels (b) and (c) and indeed of any parcels which are in thermal contact with the plate at both extremes of their motion.

Now let us look more fully at this hydrodynamic heat transport. Let us imagine that while for clarity we drew parcels (a) and (c′) or (a′) and (b) (and similarly for the others) in different locations, in fact, (c′) took the place of (a), (a′) took the place of (b), etc. for all the parcels. Then the <u>net</u> heat transfer from fluid to plate will be zero: For example, at the point of the plate adjacent to (a) and (c′) heat Q is given to the plate on 4→1 of (a) but removed from the plate on 2→3 of (c′). Hence, the thermal condition in the center of the plate is not affected on average by the average hydrodynamic entropy flow adjacent to it. In this simple picture, Q is extracted from the reservoir at $T_H$ by (b′), passed on down the plate in successive cyles, and then rejected to the reservoir at $T_C$ by (c). This result is not quite right, owing to losses and to the performance of work, but it is essentially correct for the case of a stack much shorter than the acoustic wavelength.

It is also easy to see from Fig. 2 that work will flow out of the engine. After the process 1→2, the dynamic pressure is positive while the heat flow causes the gas to expand during 2→3. After the process 3→4, the dynamic pressure is negative while the gas contracts during 4→1. The net effect is that work is done by the parcel on its surroundings, so work will flow out of the engine.

## SOME CALCULATIONS FOR A REASONABLE ENGINE

In this section we present some numerical calculations we did based on the quantitative theory outlined above and presented in detail in reference (16). These calculations were intended to serve as

guidelines for a moderately simple laboratory model of a liquid-sodium thermoacoustic engine. The actual choices of materials and temperatures are more strongly influenced by considerations of cost, simplicity, and flexibility with respect to modification than by a goal of achieving the "ultimate" prime mover. In any event, in even the simplest engine there is a competition between efficiency and work flow, which, at this stage, should not be resolved.

In working out the numerical solutions we have started with assumptions that, in our judgement, are appropriate for initial work on an actual experimental engine. As the engine should have a practical size corresponding to a half-wavelengh of about 1 m, we have chosen an operating frequency of 1 kHz. The mean pressure must also be reasonable and consistent with the strength at elevated temperatures of a cheap and readily machined construction material, stainless steel, which is also compatible chemically with liquid sodium. We chose $P_m$ = 200 bar and $T_H$ = 725°C, as well as stainless steel for the pressure vessel, even though more exotic materials and higher temperatures will be appropriate if the engine proves practical. Sodium is relatively incompressible so that the pressure amplitude can be 0.99 $P_m$ for Mach numbers less than 2 X $10^{-3}$. The plate material must be chosen to give a large value of $\sqrt{\rho_s c_s k_s / \rho_m c_p k}$, something easy to achieve for gases but not for a liquid metal. This ratio is about 5 for copper, which dissolves in liquid sodium, and about 2 for molybdenum or tungsten; thus the calculations are for plates made of tungsten. Sodium freezes at 93°C, so a reasonable choice for $T_C$ is 125°C. As we seek high work flow densities at reasonable efficiencies, we chose 300 W/cm$^2$ of heat flux density at the hot end. This heat flux, although slightly higher than the 280 W/cm$^2$ that we found was required for the maximum efficiency, is in the direction of a suitable compromise between efficiency and work flow. Under the above constraints, a search was made for optimal values of plate spacing, plate thickness, and other geometry to maximize work flow. The result of this optimization is presented in Table I. The efficiency $\eta$, the ratio of work flow to hot end heat flow, is calculated to be 0.18, so that the ratio of $\eta$ to Carnot's efficiency $\eta_c$ is 0.31.

Fortunately for experimental work, a general quality of a reasonably well optimized liquid-sodium acoustic engine, such as the one discussed here, is insensitivity to geometry. For example, an 8% decrease in distance from plates to resonator end or a 4% decrease in plate spacing decreases calculated efficiency by only 0.5%. The efficiency is also insensitive to changes in heat flux. The engine should operate well over a good range of power densities, so operation will not be seriously affected by small errors in fabrication, material properties, and the like.

TABLE I. Parameters for a reasonably optimized engine

| | |
|---|---|
| Frequency | 1000 Hz |
| Hot Temperature | 725°C |
| Cold Temperature | 125°C |
| Mean pressure | 200 bar |
| Dynamic pressure | 198 bar |
| Plate spacing | 0.037 cm |
| Plate thickness | 0.028 cm |
| Distance of hot end from tube end | 8.65 cm |
| Length of stack | 8.0 cm |
| Hot end heat flow | 300 W/cm$^2$ |
| Work flow | 55.1 W/cm$^2$ |
| $\eta$ | 0.18 |
| $\eta/\eta_c$ | 0.31 |

The temperature-dependent thermodynamic properties of liquid sodium favor higher temperature engines where $T\beta$ and $\gamma$-1 are high and viscosity low. A straightforward way of determining the relative importance of temperature-dependent effects is to examine engine performance numerically as the hot end increases in temperature. In Fig. 3 we show calculated values of $\eta/\eta_c$ vs $T_C$ for various values of $T_H$ for the 1 kHz engine. The substantial improvement in efficiency for higher temperature engines is apparent.

## PRELIMINARY MEASUREMENTS

To begin to test these ideas we have built a device resembling that of Fig. 1, but without any means for extracting work. The stack of plates is made of a single bar of molybdenum cut into plates and leaving a central rib for support using wire electric discharge machining. The plate thicknesses are 0.30 mm and the spacings between plates are 0.38 mm, comparable to the values displayed in Table I. The length of the stack is only 5.20 cm, as we wanted the engine to begin to oscillate at a reasonably low temperature. The stack just fits inside the circular resonator tube, whose internal area is 10 cm$^2$ and whose length is 106 cm; the center of the stack is 15 cm from one end of the resonator. The resonator is made of stainless steel parts welded together. Each of the two heat exchangers consists of a row of 16 stainless steel capillary tubes 1.3 mm in outside diameter with 0.2 mm wall immediately adjacent to an end of the stack. Pressurized water regulated at 125°C is pumped through the cold heat exchanger to remove heat from the engine, and electrically heated

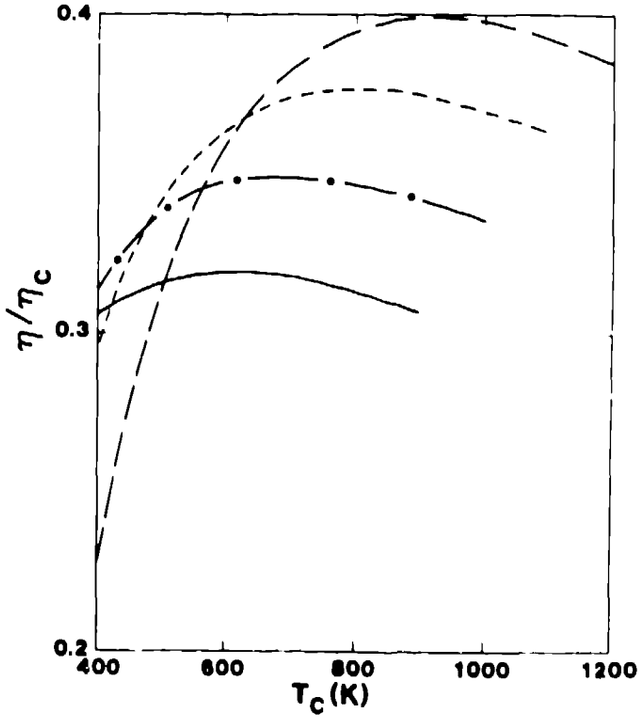


Fig. 3 - Calculated $\eta/\eta_c$ versus cold temperature (in degrees Kelvin) for the engine of Table I at various hot temperatures, and thus for various stack lengths. $T_H$ is 1300 K for the long dashes, 1200 K for the short dashes, 1100 K for the dot-dashes, and 1000 K for the solid line.

liquid sodium is pumped through the hot heat exchanger at a known temperature to supply heat to the engine.

As of the date of preparation of this manuscript, we have only the most preliminary measurements with this engine, but we present them because they demonstrate the remarkable fact that the engine works. The working instrumentation on the engine allowed us to measure the acoustic acceleration of the resonator, the temperatures at relevant points, and the flow rates of sodium and water through the two heat exchangers. From the inlet and outlet temperatures of the flowing heat exchange sodium, its flow rate, and its specific heat, we computed the rate of heat supplied to the engine $\dot{Q}$. In Fig. 4 we show $\dot{Q}$ vs. the temperature across the stack $\Delta T$. The points are values measured as described above. The solid line is the value of $\dot{Q}$ calculated from simple conduction of heat by the sodium, molybdenum, and stainless steel spanning the temperature difference. (Stray conduction from $T_H$ to room temperature is not accounted for.) We see that around $\Delta T$ = 400°C the measured $\dot{Q}$ began to increase dramatically above its value for simple conduction, as acoustically stimulated heat flow occurred. The resonator accelerometer showed that oscillations at 906 Hz began at $\Delta T$ = 350°C; by $\Delta T$ = 520°C the resonator was oscillating at high enough amplitude that the 906 Hz sound it radiated into the room was unpleasantly loud. A calculation for this geometry and frequency as described above showed that the engine should have begun to oscillate at $\Delta T$ = 260°C. The mean pressure for these measurements was 68 bar, so the acoustic pressure amplitude could have been no higher than that. At that pressure amplitude and for $\Delta T$ = 520°C the calculations showed an expected $\dot{Q}$ = 2000 W whereas the measured value was 2600 W. We do not yet understand these disagreements. Although the heat flow discrepancies could be within experimental uncertainties, the temperature descrepancies are not.

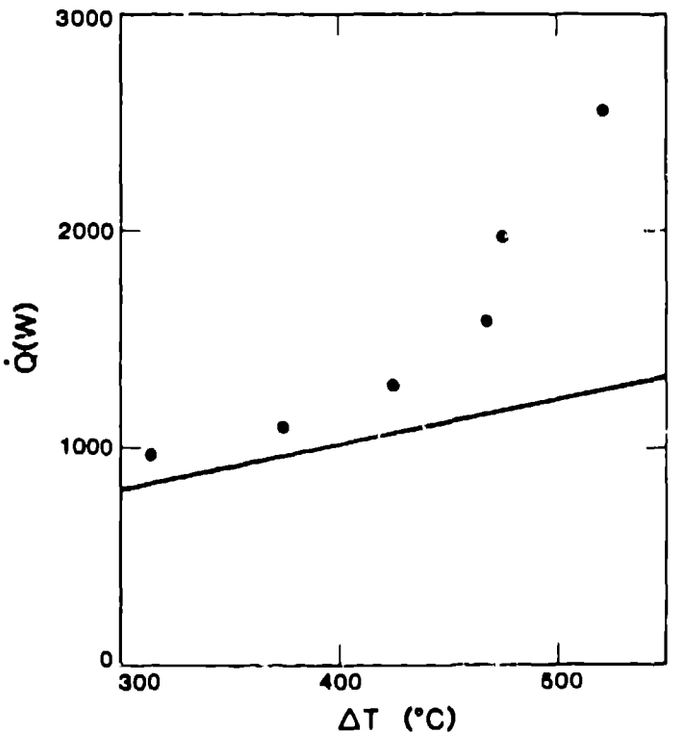


Fig. 4 - Heat flow $\dot{Q}$ into the hot end of the engine vs. temperature difference $\Delta T$ across the engine. Points are measured data; the line is a calculation of conduction only with no thermoacoustic effects.

## A MAGNETOHYDRODYNAMIC CONVERTER

We are also developing a magnetohydrodynamic (mhd) transducer to convert the acoustic power generated by the thermoacoustic engine into electric power. Our first attempt at such a converter was quite successful. The mhd transducer consisted of a rectangular channel for the sodium of thickness 1.2 cm in the direction of the 2.3 T magnetic field, width 7.6 cm in the direction of electric current flow, and length 31 cm in the direction of acoustic fluid flow, with the central 20 cm of that length actually in the magnetic field and in contact with the electrodes. Leads from the electrodes were connected to a 1:572 transformer to transform the electric power to useful voltage and current levels. The transducer was welded into the center of a 1-m long, 10-cm$^2$ cross section high Q resonator filled with sodium at 130°C. It is now well characterized both experimentally and theoretically. Such a transducer obeys

$$\Delta P = \alpha U + \beta I \qquad (13)$$

$$V = \beta U + \gamma I \qquad (14)$$

where V and I are the voltage across and current through the transducer, $\Delta P$ and U are the pressure drop across and volumetric velocity through the channel, and $\alpha$, $\beta$, and $\gamma$ are coefficients, whose measured values agree very well with calculations.

To test the transducer's efficiency in converting acoustic power to electric power, we put electric power <u>into</u> the transducer to excite the sodium on resonance at high amplitude, and the switched the transducer to a load resistor $R_L$ and let the energy stored in the acoustic resonance flow through the transducer to the load. Figure 5 shows the efficiency e, defined as the ratio of measured electrical energy delivered to the load to calculated stored acoustic energy, vs. $R_L$ and applied magnetic field. These measurements were all made at power levels of roughly 1 W; an accident destroyed the apparatus before we could try powers at the design level of 1 kW. The highest observed efficiency is about 45%. We believe we can build a more efficient transducer, by reducing the series lead resistance responsible for low efficiency at low values of $R_L$, and by changing the channel geometry to reduce the short-circuiting and effects responsible for reduced efficiency at higher $R_L$.

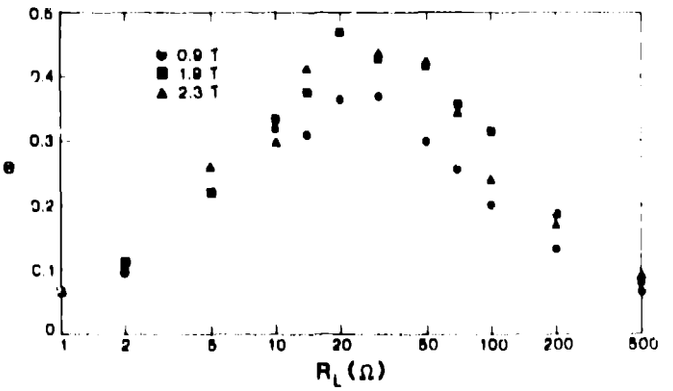


Fig. 5 - Efficiency e of the mhd transducer vs. load resistance $R_L$, for several magnetic field strengths.

## FUTURE PLANS

Although there is no acoustic-to-electric power converter in the first engine assemly, we will be able to learn about the resonator losses, the critical temperature gradient, heat exchange efficiency, and perhaps the extent of the linear acoustic regime. Meanwhile we are designing a new, more efficient mhd transducer. Next, we will at least splice together the engine assembly with the mhd transducer, to see how the engine behaves when it is producing real power and to explore the heat pumping regime of operation as well as the prime mover regime. We may have to build a dual engine, with an engine in each end of a half-wavelength resonator, to overcome unexpectedly large resonator losses.

There are also some theoretical and calculational problems we would like to work on. We suspect that mixing a little travelling acoustic wave in with the standing wave and decreasing the plate spacing will lead to higher engine efficiency by making the engine more Stirling-like and less intrinsically irreversible. We'd like to do some calculations to test this idea. Also, the idea of using radial acoustic resonances in a cylinder or sphere is appealing and should be investigated theoretically. Acoustic-to-electric conversion in such geometries would then require consideration too.

## ACKNOWLEDGEMENT

This work is supported by the Division of Advanced Energy Projects in DOE's Office of Basic Energy Sciences.

## REFERENCES

1. C. Sondhauss, Ann. Phys. (Leipzig) 79(2) 1 (1850).
2. J. W. Strutt (Lord Rayleigh), The Theory of Sound (Dover, New York, 1945), Vol. II, Secs. 322 f-i.
3. K. T. Feldman, Jr., J. Sound Vib. 7, 71 (1968).
4. N. Rott, Zh. Angew. Math. Phys. 20, 230 (1969).
5. N. Rott, Zh. Angew. Math. Phys. 24, 54 (1973).
6. N. Rott, Zh. Angew. Math. Phys. 25, 619 (1974).
7. N. Rott, Zh. Angew. Math. Phys. 26, 43 (1975).
8. N. Rott and G. Zouzoulas, Zh. Angew. Math. Phys. 27, 197 (1976).
9. G. Zouzoulas, Zh. Angew. Math. Phys. 27, 325 (1976).
10. N. Rott, Adv. Appl. Mech. 20, 135 (1980).
11. U. A. Muller and N. Rott, "Thermally Driven Acoustic Oscillations, Part VI: Excitation and Power" (preprint, 1984).
12. John Wheatley, T. Hofler, G. W. Swift, and A. Migliori, Phys. Rev. Lett. 50, 499 (1983).
13. John Wheatley, T. Hofler, G. W. Swift, and A. Migliori, J. Acoust. Soc. Am. 74, 153 (1983).
14. John Wheatley, T. Hofler, G. W. Swift, and A. Migliori, Am. J. Phys. 53, 147 (1985).
15. J. F. J. Malone, J. R. Soc. Arts (London) 79, 679 (1931).
16. G. W. Swift, A. Migliori, T. Hofler, J. C. Wheatley, J. Acoust. Soc. Am. 78, 767 (1985).